DOI: 10.1002/ejic.200800094

Plasticity in $[(R_{4-x}R^1_x)_4N]_4[Cu_4\{S_2C_2(CN)_2\}_4]$ (x = 0–4) is Molded by a Guest Cation on an Elastic Anionic Host

Biplab K. Maiti,[a] Kuntal Pal,[a] and Sabyasachi Sarkar*[a]

Keywords: Cation template / Plasticity / Elasticity / Host–guest systems / Supramolecular chemistry

The elastic anion $[Cu_4(mnt)_4]^{4-}$ {mnt = maleonitriledithiolato, $[S_2C_2(CN)_2]^{2-}$} serves as a host to a series of guest cations $[(R_{4-x}R^1_x)_4N]^+$ (R = Et, R^1 = Me; x = 0–4) to form the complexes $[(R_{4-x}R^1_x)_4N]_4[Cu_4\{S_2C_2(CN)_2\}_4]$. The molecular structural design information stored in the cation is molded to the elastic anionic host-framework through H-bonding to create a plastic supramolecular entity. The reaction of CuCl with Na_2(mnt) in a 1:1 metal/ligand ratio, followed by interaction with the respective cation, gives the cation-dependent tetranuclear host-guest assemblies $[Me_4N]_4[Cu_4(mnt)_4]$ (**1**), $[Me_3EtN]_4[Cu_4(mnt)_4]$ (**2**), $[Me_2Et_2N]_4[Cu_4(mnt)_4]$ (**3**), $[MeEt_3N]_4[Cu_4(mnt)_4]$ (**4**) and $[Et_4N]_4[Cu_4(mnt)_4]$ (**5**), which have been characterized by X-ray structural studies in the solid state. The host cavity shrinks and expands, with varying Cu···Cu separations ranging from 2.754 to 3.952 Å, to accommodate the relevant guest ion during the crystallization process. All these complexes show identical ^{13}C NMR and UV/Vis spectra in solution and their identical cyclic voltammetric redox behaviors also imply the presence of a common entity. The ESI mass spectra in acetonitrile confirm the presence of this common $\{Cu_4(mnt)_4\}$ core. The elastic $\{Cu_4(mnt)_4\}$ core participates in extensive hydrogen bonds in the presence of different quaternary cations in solution during the crystallization process and the cation determines the final shape of the anion in the solid state. Depending on the length and nature (symmetric or non-symmetric) of the alkyl groups attached to the quaternary cation, the overall geometry of the anion assumes different degrees of openness in a partially opened umbrella shape. The $\{Cu_4(mnt)_4\}$ moiety is cleaved by treatment with PPh_3 to give a monomer, which has been isolated as $[Et_4N][Cu(mnt)PPh_3]$ (**6**).

Introduction

The metal-assisted self-assembly of metallacycles, helicates, racks, ladders, grids, and cages is an impressive achievement in molecular design and assembly.[1] It has become now apparent that by proper manipulation of the noncovalent interactions between anions[2] or cations[3] the course of the assembly process may follow the chemistry of molecular information. The involvement of reversible dynamic covalent and noncovalent connections means that a particular combination of metal ion or ligand can be assembled in a process where the cation templates like a target lock or kinetic selection.[4] Such ionic recognition may lead to the binding of a guest to a host and this binding may further involve a complex interplay of subtle noncovalent interactions.[5] Numerous synthetic host–guest systems are potentially useful in separation processes, recognition, catalysis, and sensor technologies;[6] indeed, guest-exchange processes have been reported for a number of supramolecular metal–ligand hosts.[7] Synthetic chemistry has evolved traditional methods that produce only a rigid host cavity that is based on guest size selectivity. Recently, however, Raymond and co-workers have described the elasticity of a host cavity in solution where an encapsulated guest may be exchanged from the cavity by deformation of the host framework.[8] We envisioned a different situation where the plasticity of the host cavity may be melted (used in terms of plastic melting) to accommodate different guests by mapping the size and shape of the guest during the remolding process. Such a process requires disruption of the noncovalent interactions between the guest and the host during melting process whilst retaining the nature of the host framework. During this guest-exchange process the melted host (on dissolution) can regenerate an elastic relaxed host framework, which effectively remolds itself in the presence of a new guest during re-crystallization.

The discrete metallacycles to be used as hosts were synthesized on the basis of a rational ligand-directed approach.[9] We decided to use Na_2(mnt) as a chelate ligand as sulfur has the possibility of linking a soft transition metal ion in diverse bridging modes,[10–12] such as μ_2-S and μ_3-S. On the basis of the above idea we developed a series of compounds based on a partially opened umbrella-shaped tetranuclear core, $\{Cu_4mnt_4\}$, where the openness is controlled by several noncovalent interactions with the hydrogen atoms of the cation. The X-ray structures of all these

[a] Department of Chemistry, Indian Institute of Technology Kanpur,
Kanpur-208016, India
Fax: +91-512-259-7265
E-mail: abya@iitk.ac.in

Supporting information for this article is available on the WWW under http://www.eurjic.org or from the author.

complexes show the maintenance of the plasticity of the opened umbrella-shaped $\{Cu_4mnt_4\}$ core upon encapsulating tetraalkylammonium cationic species of varying sizes and shapes. Uniquely, the rigid tetranuclear complexes sever several hydrogen bonds on dissolution, thereby liberating the relaxed tetranuclear core and losing their structural plasticity. On addition of an excess of a new tetraalkylammonium cation, its hydrogen atoms impart newer forces for association with the tetranuclear core and these alter the placement of the core cations to impart a new structural motif for the tense tetranuclear core that leads to a reshaping of the fold of the umbrella on recrystallization. Such reversibility shows the plasticity of the tetranuclear core when accommodating a new cation. This process is reversible and different shapes of the partially opened umbrella can be molded by different guest cations. The tetranuclear core can be ruptured in solution by addition of PPh_3, which acts as a blocker to prevent Cu–S bond formation and yields $[Et_4N][Cu(mnt)PPh_3]$.

Previously known structurally characterized tetranuclear Cu^I complexes such as $[Cu_4(dtc)_4]$,[13] $[Cu_4(dtp)_4]$,[14] $[Cu_4(S_2CC_7H_7)_4]$,[15] and $[Cu_4(i\text{-}mnt)_4]^{4-}$[16] (dtc: dithiocarbamato, dtp: dithiopropionato, *i*-mnt: isomaleonitriledithiolato, mnt: maleonitriledithiolato) have in common that their copper atoms are disposed almost at the vertices of a distorted tetrahedron. Compounds **1**–**5** are the first structurally characterized tetranuclear Cu^I complexes with four dianionic 1,2-dithiolato ligands, which results in the formation of anionic species. An X-ray-structural analysis shows that the cations used as a guest in **1**–**5** play a decisive role in molding the final shape of the tetranuclear anionic frame. The plasticity of the $\{Cu_4(mnt)_4\}$ framework only exists in the solid state − the ^{13}C NMR and UV/Vis spectra and cyclic voltammetric studies indicate the existence of a common unit in solution, namely tetranuclear $\{Cu_4(mnt)_4\}$, as determined by ESI mass spectrometry.

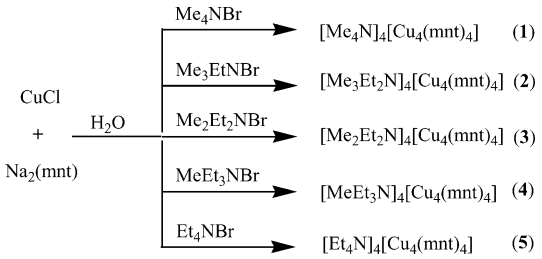

Scheme 1. Schematic representation of the cation-assisted self-assembly process.

Results and Discussion

Synthesis

The tetranuclear host–guest assemblies **1**–**5** were synthesized by treating CuCl with $Na_2(mnt)$ in a 1:1 molar ratio in water. The desired yellowish-orange compound precipitated upon addition of an aqueous solution of the respective quaternary ammonium bromide (cations Me_4N^+, Me_3EtN^+, $Me_2Et_2N^+$, $MeEt_3N^+$, and Et_4N^+; Scheme 1) in high yield. Interestingly, addition of a cation such as Bu_4N^+ gave the trinuclear complex $[Bu_4N]_3[Cu_3(mnt)_3]$[17] instead.

Compounds **1**–**5** isolated from the aqueous reaction medium and recrystallized from acetonitrile/diethyl ether were found to be structurally identical, as confirmed by comparing the respective pairs of XRD patterns (see Figure S11 in the Supporting Information) and by checking their melting points. These results assured us that the single crystals used in the diffraction analyses retained the tetranuclear form isolated originally from the aqueous medium. All these compounds can easily be interconverted simply by dissolving one of them in CH_3CN, adding an excess of the alternate cation, and precipitating the new complex by adding diethyl ether (Scheme 2). These core conversions were confirmed by measuring the unit cell dimensions and melting point. Complexes **1**–**5** are smoothly converted into $[Cu(mnt)(PPh_3)]^-$ with the respective counter cation upon treatment with four equivalent of PPh_3 in dichloromethane (Scheme 3). Compounds **1**–**5** are highly susceptible towards oxygen in solution, which leads to the oxidation of the copper(I) ion, whereas **6** is more stable and reacts only slowly with oxygen in solution. On aging, all these complexes with a $\{Cu_4mnt_4\}$ core slowly lose an mnt^{2-} anion to form $[Cu^{II}(mnt)_2]^{2-}$, along with a more stable cubane core,[11,12] especially in the presence of traces of air.[16] This reaction can be followed by electronic spectroscopy (see Figure S1 in the Supporting Information).

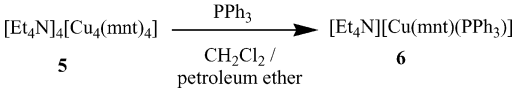

Scheme 2. Transformation from tetramer to monomer.

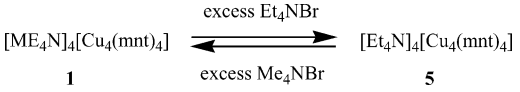

Scheme 3. Interconversion between **1** and **5**.

Solution UV/Vis Study

The electronic absorption spectra (Figure 1) of **1**–**5** in acetonitrile are identical and superimposable, with a common charge-transfer band at 377 nm.

This suggests that **1**–**5** generate a common species in solution upon breaking of all the hydrogen-bonding interactions. However, the released tetramer appears to be stable and further fragmentation to yield a monomer, dimmer, or other forms, which may remain in equilibrium, cannot be detected. A charge-transfer band is observed at 372 nm for **6**.

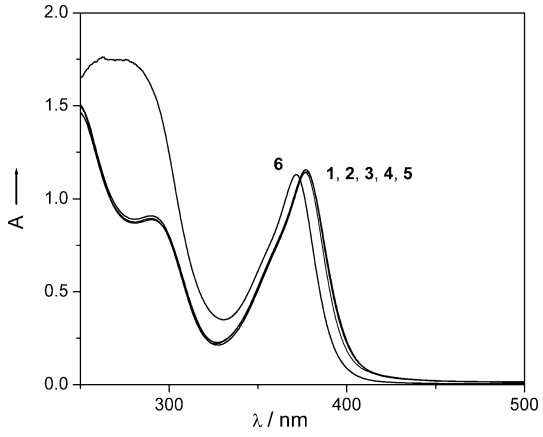

Figure 1. The electronic absorption spectra of **1** (0.25×10^{-4} M), **2** (0.25×10^{-4} M), **3** (0.25×10^{-4} M), **4** (0.25×10^{-4} M), **5** (0.25×10^{-4} M), and **6** (1×10^{-4} M) in CH_3CN solution.

Electrochemistry

Cyclic voltammetric analysis was performed to determine the number of electroactive copper-containing species as the oxidation of copper(I) should vary in different environments. Thus, the presence of a monomer, dimmer, or tetramer, etc. will lead to the appearance of different metal oxidation based peak potentials. Any geometry changes due to the presence of a further quaternary cation were avoided by using KPF_6 as the supporting electrolyte and performing the measurements in acetonitrile to maintain the identity of the species detected by electronic spectroscopy. CV was performed for **1**–**5** in CH_3CN solution containing 0.1 M KPF_6 as the supporting electrolyte. Ferrocene was used as an internal standard and the potentials were referenced to the Ag/AgCl electrode. Electrochemical measurements at platinum and glassy carbon working electrodes gave similar results for complex **5** (Figure S2 in the Supporting Information).

Complexes **1**–**5** exhibit identical electrochemical responses, a result which is in agreement with the results of the electronic spectral study. The CV of all tetranuclear complexes (Figure 2) show two anodic peaks (E_{pa}) at 0.22 and 0.32 V vs. Ag/AgCl. Both these processes have the corresponding cathodic peaks (E_{pc}) at 0.15 and 0.24 V, respectively, which suggests that we are dealing with two sequential one-electron oxidations (ΔE = 70 mV in each case). The first oxidation process overlaps with the second oxidation process. Differential pulse polarography (DPP) of these species showed oxidation processes at 0.19 and 0.27 V, close to the $E_{1/2}$ values of the two processes found in the CV studies. Cyclic voltammetry of compound **5** in CH_3CN (0.2 M, supporting electrolyte, KPF_6) at scan rates of 50–400 mV s^{-1} showed two peaks at the same positions but with current intensities that are strongly affected by the scan rate (Figure S2 in the Supporting Information). The intensities and peak positions are independent of the number of scans (see Figure S3 in the Supporting Information). These oxidations are copper-centered and presumably not due to the oxidation of μ_1-S/μ_2-S bridging sulfur.

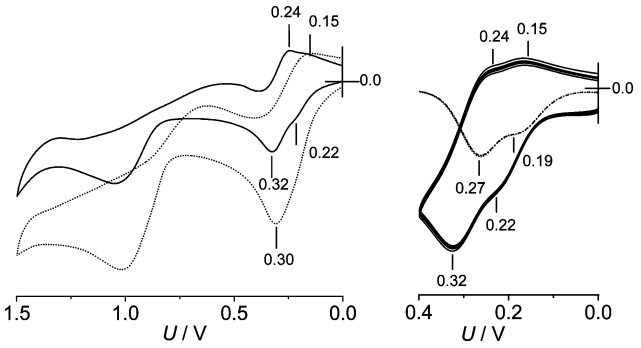

Figure 2. Left: full-scan CV spectra of **5** (1×10^{-3} M; solid line) and **6** (4×10^{-3} M; broken line); right: CV (solid line) and DPP (broken line, current height reduced by 1/3 with respect to CV) of **1**–**5**. All spectra were recorded at a scan rate of 100 mV s^{-1} over the potential range of interest (0 to +0.40 V) in acetonitrile with KPF_6 as the supporting electrolyte.

It is known that metal sulfido complexes can incorporate elemental sulfur to form polysulfide complexes,[16] therefore we added one equivalent of elemental sulfur to a solution of **5** during the CV study. The color of the solution darkened from yellow to orange but there was no change in the redox peak positions in CV or DPP compared to those found for pure **5**. The addition of one equivalent of PPh_3 to the solution caused the color to revert to that of **5**. The formation of PPh_3S in this reaction was subsequently confirmed. A similar reaction between a polysulfido copper complex and PPh_3 has been reported,[16] therefore the species generated upon addition of elemental sulfur in the present case must be similar, with the coordinated sulfide ligand being converted into a polysulfide from which sulfur can be abstracted by PPh_3 to yield PPh_3S. As the peak position remains unaltered upon addition of elemental sulfur, these redox processes cannot be related to copper as in that case the position of the sulfide-dependent redox peak should change due to formation of the polysulfide entity. The ready aerobic oxidation of these complexes indicates the ease of oxidation of Cu^I. The only information that can be extracted from this study, therefore, is the presence of common copper-containing species in solution for all complexes.[18] However, the presence of two structurally different species containing copper(I) in two different environments, or one complex containing two nonequivalent copper(I) centers, both of which could account for these two successive oxidation processes, cannot be differentiated. The choice of species in solution has been narrowed down however. Compound **6** displays one anodic peak, E_{pa}, at 0.30 V vs. Ag/AgCl due to an irreversible oxidation.

NMR Spectroscopy

The ^{13}C NMR spectra of all complexes were recorded in argon-purged [D_6]DMSO and in CD_3CN; key peaks are listed in Table 1. CD_3CN masks the CN peak of the mnt^{2-}

ligand but it is nevertheless used, along with DMSO, as a common solvent for most of the solution studies. NMR measurements were carried out with varying concentrations (30 and 50 mM) of complex **1** to the saturation limit (ca. 50 mM) to identify the presence of intermediate species due to concentration-dependent equilibria. The ^{13}C NMR spectra were identical in both cases.

Table 1. ^{13}C NMR spectroscopic data of all compounds.

Compd.	Ligand (mnt) CN	C=C	CH_3	Cation α-CH_2	β-CH_3
1	124.67	120.12	59.48	–	–
2	124.67	120.12	51.73	60.54	8.16
3	124.67	120.12	48.99	58.04	7.83
4	124.67	120.12	50.3	53.7	11.3
5	124.67	120.12	–	51.49	7.15
6	125.21	120.86	–	51.55	7.16

The ^{13}C NMR spectra of **1**–**5** in [D_6]DMSO (Table 1) show two resonances at δ = 120.12 ppm for C=C carbon atoms and at δ = 124.67 ppm for the CN moiety. The CN and C=C groups present in the coordinated mnt^{2-} ligand in **1**–**5** are in different structurally imposed environments in the solid, which suggested to us that they should display four ^{13}C peaks; only two ^{13}C peaks are observed in [D_6]-DMSO. This is due to a rapid positional change of the sulfur atoms, where Cu–S bonds arising due to μ_1-S and μ_2-S bridging interchange their positions faster than the NMR timescale, which means that the sulfur atoms of the mnt^{2-} ligand are equivalent in solution on the NMR timescale (clockwise and anticlockwise copper–sulfur binding modes).[17] In contrast, only a clockwise or anticlockwise structure is found in the solid state. The appearance of concentration-independent CN and C=C peaks at the same position for all tetramers shows that the coordinated mnt^{2-} ligand is in an identical environment in solution on the NMR timescale. The results of the electronic spectroscopy and CV studies have allowed us to narrow the possible species in solution down to least two, and the ^{13}C NMR results reduces that possibility still further to enantiomeric forms.[17]

The NMR spectrum of **6** is noticeably different. Thus, the CN and C=C signals are both shifted down-field to δ = 125.21 and 120.86 ppm, respectively, due to a change in the coordination mode of the dithiolene and PPh_3 ligands. The CN signal is less shifted than C=C as it is further away from the coordination site. The ^{13}C NMR assignment of the respective cations of **1**–**6** in [D_6]DMSO is straightforward (Table 1). The ^{13}C NMR spectrum of **6** in [D_6]DMSO also exhibits resonances due to the PPh_3 moiety

Electrospray Mass Spectrometry

Self-assembled supramolecular host-guest complexes have been characterized by electrospray ionization mass spectrometry.[19] The high symmetry inherent to most supramolecular assemblies can lead to difficulties in assessing the exact stoichiometry of host-guest complexes by solution-based characterization methods. Mass spectrometry, however, allows for a convenient assessment of the exact stoichiometry based on the mass and isotopic composition of the ions observed. The ESI mass spectra in the negative ion mode were acquired under mild conditions using a needle voltage of 2.5 kV and a cone voltage of 40 V. The ESI mass spectrum of complex **5** in CH_3CN shows a signal at *m/z* 1203.99 due to $[Et_4N]_3[Cu_4(mnt)_4]^-$ along with fragments assigned to $[Et_4N]_2[Cu_3(mnt)_3]^-$, $[Et_4N][Cu_2(mnt)_2]^-$, and $[Cu(mnt)]^-$ at *m/z* 870.90, 538.10, and 203, respectively (Figure 3).

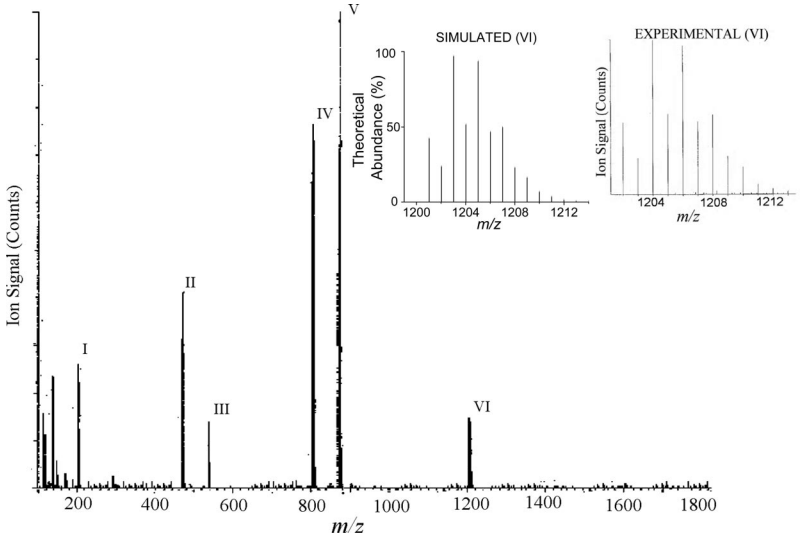

Figure 3. Electrospray mass spectrum of **5** in CH_3CN. The ion signals displayed correspond to $[Cu(mnt)]^-$ (I) at *m/z* 203, $[Et_4N][Cu^{II}(mnt)_2]^-$ (II) at *m/z* 474.35, $[Et_4N][Cu_2(mnt)_2]^-$ (III) at *m/z* 538.10, $[Et_4N]_2[Cu_8(mnt)_6]^{2-}$ (IV) at *m/z* 803.66, $[Et_4N]_2[Cu_3(mnt)_3]^-$ (V) at *m/z* 870.90, and $[Et_4N]_3[Cu_4(mnt)_4]^-$ (VI) at *m/z* 1203.99 (parent ion peak). The experimental and theoretical isotopic distribution patterns of VI are shown in the inset.

Changing the needle voltage to 3.5 kV whilst keeping cone voltage the same resulted in fragmentation of all the complex into the $[Cu(mnt)]^-$ ion (m/z = 203). The identity of the tetramer and monomer forms was confirmed by comparing these m/z peaks with their simulated isotopic distribution pattern using the program ISOPRO3.0.[20] The ESI mass spectra of **1**–**4** show similar fragmentation patterns (see Supporting Information). In addition, due to the presence of traces of oxygen,[16] mass fragments assignable to $[Cu^{II}(mnt)_2]$ and $[Cu_8(mnt)_6]$ species are observed. The parent ion peak of **6**, which appears at m/z 465, is due to $[Cu(mnt)(PPh_3)]^-$ and the peak at m/z 203 is again due to $[Cu(mnt)]^-$ formed by loss of PPh_3 from the former. The PPh_3-bound Cu^I center in **6** resists aerial oxidation and so species like $[Cu^{II}(mnt)_2]$ and $[Cu_8(mnt)_6]$ were not detected in its ESI mass spectrum. The presence of the parent tetrameric $\{Cu_4(mnt)_4\}$ unit as a common entity in the low energy ESI mass spectra of all the complexes strongly support its existence in solution. Application of a slightly higher needle voltage to all these complexes results in the presence of only a monomeric unit. The existence of a common tetrameric unit in solution therefore reveals the identity of the common species found by ^{13}C NMR, electronic spectroscopy, and by CV. This suggests that complexes **1** to **5** form a common, relaxed tetranuclear species on dissolution.

Solid-State Structure of $[Me_4N]_4[Cu_4(mnt)_4]$ (1)

The structure of the anion in **1** is illustrated in Figure 4 and selected bond lengths and angles are provided in the corresponding figure caption. Compound **1** crystallizes in the monoclinic system, space group $C2/c$. The asymmetric unit of **1** contains four half tetramethylammonium cations and one half of a $[Cu_4(mnt)_4]$ anion. One of the four $[Me_4N]^+$ cations is disordered. The N atom of this cation suffers positional disorder at a special position and it was refined using a negative part instruction. This $[Me_4N]^+$ cation is located inside the cavity of the anion host. The four Cu^I ions and mnt ligands form a discrete tetranuclear complex in which each mnt ligand forms a μ_1-S bond to a Cu atom and a μ_2-S bond to the same Cu atom to form a five-membered chelate ring.[21] This mnt ligand further binds to an adjacent Cu atom to build a Cu_4S_4 eight-membered ring. The average S···S bite distance in mnt is 3.353 Å and the average S–Cu–S angle is 96.8°.[11] The tetrameric unit contains a central Cu_4S_4 eight-membered ring comprising alternate copper and sulfur atoms. This octameric ring is nonplanar and is arranged in a crown-like configuration.[22] Each copper atom is coordinated to three sulfur atoms (one μ_1-S and two μ_2-S) and the copper atoms are displaced by 0.244 (Cu1) and 0.307 Å (Cu2) from the S_3 basal plane in a distorted trigonal planar geometry. The Cu–S distance[11,12,23,24] (2.242 Å) associated with the five-membered chelate ring is slightly larger than the bridging Cu–S distance (2.211 Å). However, the four Cu atoms can be considered as planar with the S atoms alternating above and below the plane [four μ_2-S atoms are located above the plane at a distance of 0.755 Å (S1) and 0.882 Å (S3) and four μ_1-S atoms are located below the plane at a distance of 1.954 Å (S1) and 1.849 Å (S4)]. The overall dimensions and shape of the core of the macrocyclic entity can be extracted by considering the four coplanar metal ions as the hypothetical corners of a quadrilateral. The four Cu–Cu–Cu angles (two pairs; 86.8° and 93.2°) are close to 90° but the separations between two adjacent copper atoms are not identical (two pairs of opposite distance; 2.875 and 3.087 Å) therefore the molecule contains a nearly perfect rectangular-planar arrangement. The four {Cu(mnt)} building blocks assemble in a clockwise fashion and these units are connected through four S atoms with Cu–S–Cu angles (two pairs) of 88.3° and 80.4°. The four Cu(mnt) planes are not co-planar with the Cu_4 plane but deviate (two pairs) by 65.1° and 59.9° from this plane; the two {Cu(mnt)} planes approach each other with angles of 71.7° and 83.7°. Thus, the structure of this cyclic tetramer resembles a partly opened umbrella and exhibits C_2 symmetry.

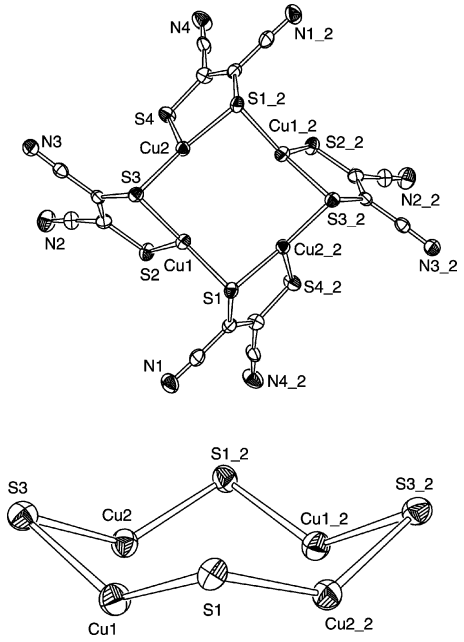

Figure 4. Structure (ORTEP drawing) of the anionic unit (top) and Cu_4S_4 core (bottom) of **1**. Thermal ellipsoids are drawn at the 50% probability level. Selected bond lengths [Å] and angles [°]: Cu1–S1 2.2087(14), Cu1–S3 2.2411(14), Cu1–S2 2.2469(13), Cu2–S3 2.2117(14) Cu2–S4 2.2565(13), Cu1···Cu2 2.8755(11); S3–Cu1–S2 97.09(5), S4–Cu2–Cu1 119.97(4), S3–Cu2–S4 121.78(5), S3–Cu2–Cu1 50.22(4), S1–Cu1–S3 135.04(5), S1–Cu1–S2 121.88(5), S1–Cu1–Cu2 131.46(4), S3–Cu1–Cu2 49.33(4), S2–Cu1–Cu2 99.62(4), Cu2–S3–Cu1 80.45(4).

Solid-State Structure of $[Me_3EtN]_4[Cu_4(mnt)_4]$ (2)

The structure of the anion in **2** is illustrated in Figure 5 and selected bond lengths and angles are provided in the corresponding figure caption. Compound **2** crystallizes in the triclinic system, space group $P\bar{1}$. The asymmetric unit of **2** contains four trimethylethylammonium cations and one

$[Cu_4(mnt)_4]$ anion. One of the four $[Me_3EtN]^+$ cations is located inside the cavity of the anion host. The chelating coordination mode, ligand orientation, and Cu–S distances in the anion of **2** are similar to those found in **1** even though its size and shape are quite different to those of **1**. The four pseudo-trigonal copper centers are displaced from the S_3-basal plane by 0.157 (Cu1), 0.178 (Cu2), 0.210 (Cu3), and 0.106 Å (Cu4) can be considered to form a plane with the S atoms alternating above and below this plane [four μ_2-S atoms are located above the plane at a distance of 0.381 (S1), 0.973 (S3), 0.576 (S5), and 1.047 Å (S7) and four μ_1-S atoms are located below the plane at a distance of 1.435 (S2), 1.865 (S4), 1.775 (S8), and 1.775 Å (S6)]. The metal-defined quadrilateral in **2** is unsymmetrical in shape with four different Cu···Cu separations of 3.641, 2.846, 3.905, and 2.753 Å and four Cu–Cu–Cu angles of 76.8°, 93°, 79.7°, and 88.9°. The four {Cu(mnt)} building blocks are connected through four S atoms with Cu–S–Cu angles of 110.3°, 79.7°, 125.2°, and 76.8°. The four {Cu(mnt)} planes are not co-planar with the Cu_4 plane but deviate by 62.9°, 55.3°, 57.8°, and 41.4° from this plane; the two {Cu(mnt)}planes approach each other with angles of 86.4°, 47.5°, 58.5°, and 87.7°. Thus, the structure of this cyclic tetramer resembles a partly opened umbrella and exhibits C_1 symmetry.

Solid-State Structure of $[Me_2Et_2N]_4[Cu_4(mnt)_4]$ (3)

The structure of the anion in **3** is illustrated in Figure 6 and selected bond lengths and angles are provided in the corresponding figure caption. Compound **3** crystallizes as tetrameric units in the monoclinic system, space group $P2_1/c$. The asymmetric unit of **3** contains four diethyldimethylammonium cations and one $[Cu_4(mnt)_4]$ anion. One of the four $[Me_2Et_2N]^+$ cations is located inside the cavity of the anion host. The bite distance, bite angles, and Cu–S distances are similar to those in **1**. Interestingly, the binding mode and relative orientation (anticlockwise) of the mnt groups are opposite to those in **1**, which suggests that the counteraction ($Me_2Et_2N^+$) changes the conformation (size and shape) of the anion of **3** from that in **1**. The four almost

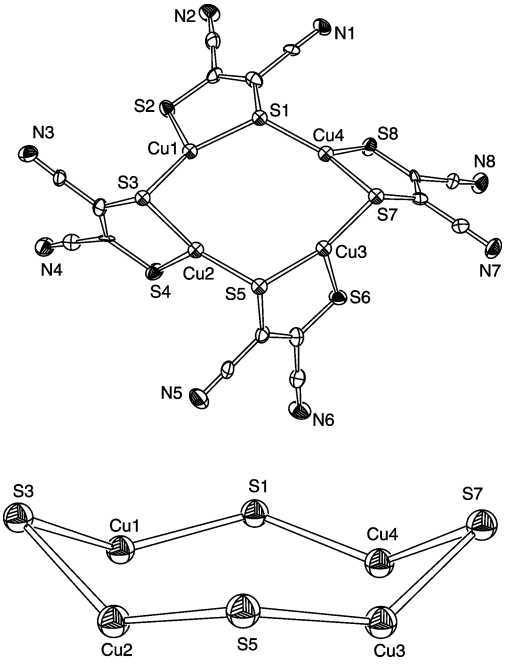

Figure 5. Structure (ORTEP drawing) of the anionic unit (top) and Cu_4S_4 core (bottom) of **2**. Thermal ellipsoids are drawn at the 50% probability level. Selected bond lengths [Å] and angles [°]: Cu1–S3 2.202(2), Cu1–S1 2.219(3), Cu1–S2 2.2403, Cu2–S5 2.196(3), Cu1···Cu2 2.8464(17), Cu2–S4 2.240(3), Cu2–S3 2.242(2), Cu3–S7 2.205(3), Cu3–S5 2.239(3), Cu3–S6 2.245(3), Cu3···Cu4 2.7539(17), Cu4–S1 2.180(3), Cu4–S7 2.229(2), Cu4–S8 2.236(3); Cu3–S7–Cu4 76.80(8), Cu4–S1–Cu1 125.22(11), Cu1–S3–Cu2 79.64(8), Cu2–S5–Cu3 110.35(10), S3–Cu1–S1 138.17(9), S3–Cu1–S2 124.24(9), S1–Cu1–S2 95.96(9), S3–Cu1–Cu2 50.80(7), S1–Cu1–Cu2 110.87(8), S2–Cu1–Cu2 133.46(8), S5–Cu2–S4 126.07(10), S5–Cu2–S3 135.49(10), S4–Cu2–S3 96.38(9), S5–Cu2–Cu1 123.20(8), S4–Cu2–Cu1 99.70(8), S3–Cu2–Cu1 49.56(6), S7–Cu3–S5 137.76(10), S7–Cu3–S6 123.31(10), S5–Cu3–S6 96.04(9), S7–Cu3–Cu4 51.99(7), S5–Cu3–Cu4 123.03(8), S6–Cu3–Cu4 120.32(8), S1–Cu4–S7 135.33(10), S1–Cu4–S8 126.02(10), S7–Cu4–S8 97.92(9), S1–Cu4–Cu3 113.97(8), S7–Cu4–Cu3 51.21(7), S8–Cu4–Cu3 105.83(8).

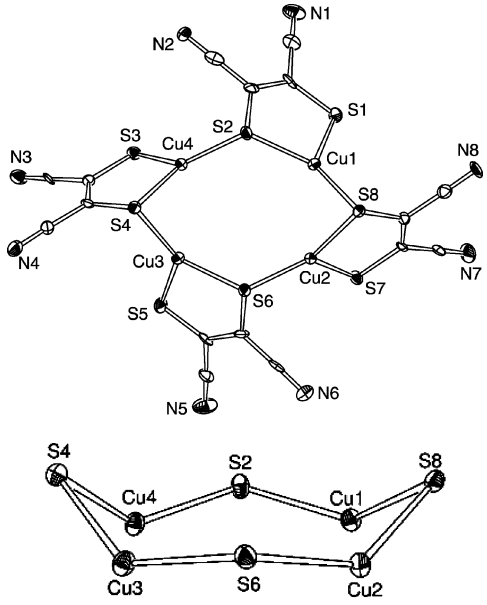

Figure 6. Structure (ORTEP drawing) of the anionic unit (top) and Cu_4S_4 core (bottom) of **3**. Thermal ellipsoids are drawn at the 50% probability level. Selected bond lengths [Å] and angles [°]: Cu1–S8 2.213(2), Cu1–S2 2.231(2), Cu1–S1 2.247(2), Cu1···Cu2 2.7840(15), Cu2–S6 2.196(2), Cu2–S8 2.230(2), Cu2–S7 2.246(2), Cu3–S4 2.203(2), Cu3–S6 2.232(2), Cu3–S5 2.233(2), Cu3···Cu4 2.7824(15), Cu4–S2 2.194(2), Cu4–S3 2.233(2), Cu4–S4 2.236(2); S8–Cu1–S2 133.63(8), S8–Cu1–S1 127.24(8), S2–Cu1–S1 95.58(8), S8–Cu1–Cu2 51.48(6), S2–Cu1–Cu2 111.32(7), S1–Cu1–Cu2 136.04(7), S6–Cu2–S8 135.59(8), S6–Cu2–S7 126.49(8), S8–Cu2–S7 96.78(8), S6–Cu2–Cu1 117.60(7), S8–Cu2–Cu1 50.94(6), S7–Cu2–Cu1 102.74(7), S4–Cu3–S6 131.65(8), S4–Cu3–S5 129.97(8), S6–Cu3–S5 96.41(8), S4–Cu3–Cu4 51.72(6), S6–Cu3–Cu4 113.81(7), S5–Cu3–Cu4 127.60(7), S2–Cu4–S3 132.98(8), S2–Cu4–S4 128.79(8), S3–Cu4–S4 96.83(8), S2–Cu4–Cu3 115.02(7), Cu1–S8–Cu2 77.59(7), Cu4–S2–Cu1 126.56(10), Cu3–S4–Cu4 77.62(7), Cu2–S6–Cu3 124.53(9), S3–Cu4–Cu3 101.89(7), S4–Cu4–Cu3 50.65(6).

trigonal planar Cu centers can be considered as being nearly rectangular [the four Cu–Cu–Cu angles (91.6°, 87.7°, 92.3°, and 88.4°) are close to 90° and the opposite distances between two adjacent copper atoms are nearly identical (3.952, 2.784, 3.919, and 2.782 Å)]. Eight S atoms alternate above and below this rectangle, with four μ_2-S atoms located above the rectangle at a distance of 0.457 (S2), 1.216 (S4), 0.399 (S6), and 1.088 Å (S8) and four μ_1-S atoms located below the plane at a distance of 1.389 (S1), 1.536 (S3), 1.616 (S5), and 1.700 Å (S7). The four {Cu(mnt)} building blocks are connected through bridging S atoms with Cu–S–Cu angles of 126.6°, 77.6°, 124.5°, and 77.5°. The four {Cu(mnt)} planes are not co-planar with the Cu_4 plane but deviation from it by 56.8°, 47.6°, 58.5°, and 39.9°; the two {Cu(mnt)} planes approach each other with angles of 82.4°, 88.9°, 46.3°, and 45.5°. Thus, the structure of this cyclic tetramer resembles a partly opened umbrella and exhibits approximate C_2 symmetry.

Solid-State Structure of $[MeEt_3N]_4[Cu_4(mnt)_4]$ (4)

The molecular structure of **4** was determined by single-crystal X-ray diffraction study. However, the quality of the crystal was poor[25]and this complex suffers from serious disorder of the cationic part, which prevents a discussion of the metrical parameters of the complex. However, from the crystal data, the basic structure of the anion in **4** similar to that of **3**.

Solid-State Structure of $[Et_4N]_4[Cu_4(mnt)_4]$ (5)

The structure of the anion in **5** is illustrated in Figure 7 and selected bond lengths and angles are provided in the corresponding figure caption. Compound **5** crystallizes as tetrameric units in the tetragonal system, space group *P*4/*n*. The asymmetric unit of **5** contains four quarters of a tetraethylammonium cation and one quarter of a $[Cu_4(mnt)_4]$ anion. One of the four $[Et_4N]^+$ cations is disordered over the carbon atoms and was refined with the free part instruction. The larger countercation in this complex helps to change the host conformation of **5** from that in **1**. The four trigonal-planar Cu centers can be considered as forming a square with four identical Cu–Cu–Cu angles (90°) and four identical (3.865 Å) Cu···Cu separations. Eight S atoms alternate above and below this square, with four μ_2-S atoms located above it at a distance of 0.540 Å and four μ_1-S atoms located below it at a distance of 1.249 Å. The four {Cu(mnt)} building blocks are connected through four S atoms with four identical Cu–S–Cu) angles of 122°. The four {Cu(mnt)} planes are not co-planar with the Cu_4 plane but deviate from it by 36.4°; the two {Cu(mnt)} planes approach each other with an angle 49.7°. Thus, the structure of this cyclic tetramer resembles a partly opened umbrella and exhibits C_4 symmetry.

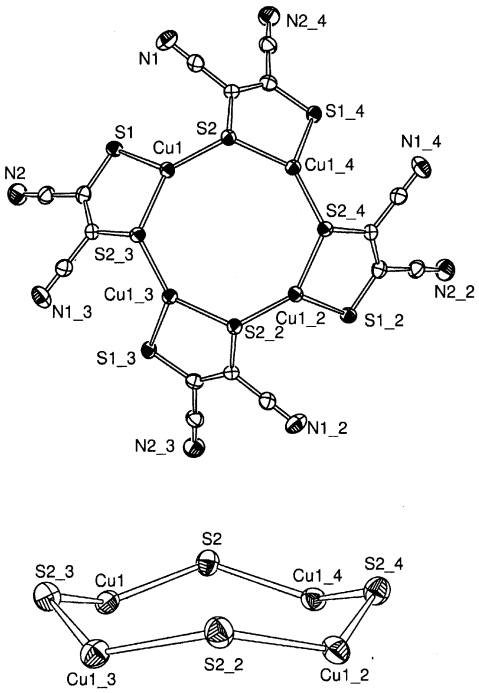

Figure 7. Structure (ORTEP drawing) of the anionic unit (top) and Cu_4S_4 core (bottom) of **5**. Thermal ellipsoids are drawn at the 50% probability level. Selected bond lengths [Å] and angles [°]: Cu1–S2 2.1801(19), Cu1–S1 2.2215(19); S2–Cu1–S1 131.33(7).

Solid-State Structure of $[Et_4N][Cu(mnt)(PPh_3)]$ (6)

The structure of the anion in **6** is illustrated in Figure 8 and selected bond lengths and angles are provided in the corresponding figure caption. Compound **6** crystallizes in the monoclinic system, space group $P2_1/n$. The asymmetric unit of **6** contains one tetraethylammonium cation and one $[Cu(mnt)PPh_3]$ anion. The complex has C_1 symmetry. The copper atom is coordinated to one P and two μ_1-S atoms in a trigonal planar geometry. The mnt ligand has two distinct S atoms, with an S···S distance of 3.342 Å and an S–Cu–S angle of 97.8°. The Cu–S bond length is 2.217 Å and Cu–P bond length[26] is 2.168 Å.

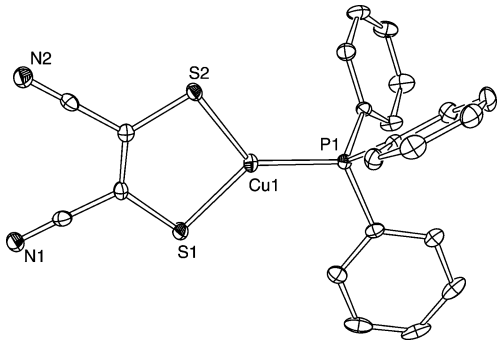

Figure 8. Structure (ORTEP drawing) of the anionic unit of **6**. Thermal ellipsoids are drawn at the 50% probability level. Selected bond lengths [Å] and angles [°]: Cu1–P1 2.1683(8), Cu1–S2 2.2166(9), Cu1–S1 2.2176(8); P1–Cu1–S2 128.77(3), P1–Cu1–S1 133.34(3), S2–Cu1–S1 97.81(3).

IR Spectroscopy

The IR spectra of **1**–**6** show the presence a ν(CN) stretching band[11,17] at 2190 cm^{-1} and bands due a ν(Cu–S) stretch in the far IR region below 300 cm^{-1}. A detailed vibration analysis was not attempted but the simple pattern of the IR band due to the Cu–S linkages shows some interesting features. The appearance of the band in the range 276–280 cm^{-1} is due to the interaction of the three-coordinate copper–sulfur bond.[27] Figure S12 (see Supporting Information) shows the variation of the ν(Cu–S) absorption due to the structural variations in **1**–**6**. This absorption appears at 280 cm^{-1} (m) in **1**, 278 cm^{-1} (s), with a shoulder at 273 cm^{-1}, in **2**, 276 cm^{-1} (s), with a shoulder at 269 cm^{-1}, in **3**, 278 cm^{-1} (s), with a shoulder at 285 cm^{-1}, in **4**, 279 cm^{-1} (s) in **5**, and 277 cm^{-1} (s) in **6**. This trend reflects the shape of the $\{Cu_4S_4\}$ core structure in the solid state. Thus, the regular symmetric $\{Cu_4S_4\}$ core in **1** and **5** shows a single ν(Cu–S) band whereas the dissymmetric cores found in **2**–**4** result in a band with another band as shoulder.

Hydrogen Bonding

The hydrogen atoms of the tetraalkylammonium cations are extensively involved in hydrogen bonds[28] with the S and N atoms of the coordinated mnt ligand. These hydrogen bonds are like spokes and control the final topology of the complex anion as a reversely held, partly opened umbrella where the N atom of a sheet-anchored cation is placed at the focal point and the $\{Cu_4S_4\}$ crown ring forms the outer rim. There is another important position of another cation just on top of the other face of the partly opened umbrella. The main interactions are from the hydrogen atoms present in the alkyl groups of these two cations and the sulfurs of the mnt ligands. The hydrogen bonds arising from these two oppositely placed (one inside the partly opened umbrella and the other outside the face of the umbrella) cations are like a bunch of spokes that control the opening or closing of the $\{Cu_4S_4\}$ core. The even or odd number of carbon atoms of the chain in the alkyl groups of the quaternary cation further controls the symmetry or dissymmetry of the $\{Cu_4\}$ core. Thus, the two sheet-anchored Me_4N^+ cations in **1** lie above and below the host framework and methyl hydrogen atoms are only involved in hydrogen-bond formation with the S-atoms of the host-framework ($d_{C–S}$ = 3.64–4.01 Å and ∠C–H···S = 114–161°), as shown in Figure 9. These distances and angles indicate weak hydrogen bonding.[28,29] In addition, the other cations (total 18) present in the lattice are also involved in hydrogen bonds with either S or N or show both C–H···S ($d_{C–S}$ = 3.36–4.01 Å and ∠C–H···S = 112–171°) and C–H···N ($d_{C–N}$ = 3.16–3.74 Å and ∠C–H···N = 103–177°) interactions.

The Me_3EtN^+ cation in **2** lies above and below the host framework and forms weak C–H···S interactions ($d_{C–S}$ = 3.52–4.02 Å and ∠C–H···S = 125–172°) with the S atoms of this framework, as shown in Figure 9. The host framework is further stabilized by other cations present in the lattice (total 18 cations) by C–H···S ($d_{C–S}$ = 3.63–4.02 Å and ∠C–H···S = 118–176°) and C–H···N ($d_{C–N}$ = 3.12–3.83 Å and ∠C–H···N = 110–177°) hydrogen-bonding interactions. These bonds play a key role in shaping the different supramolecular topology of **2**.

A different structural topology is observed for **3** in comparison with **1** or **2** due to the presence of a different counter-cation. The host framework in **3** is stabilized by C–H···S ($d_{C–S}$ = 3.65–4.01 Å and ∠C–H···S = 112–171°) and

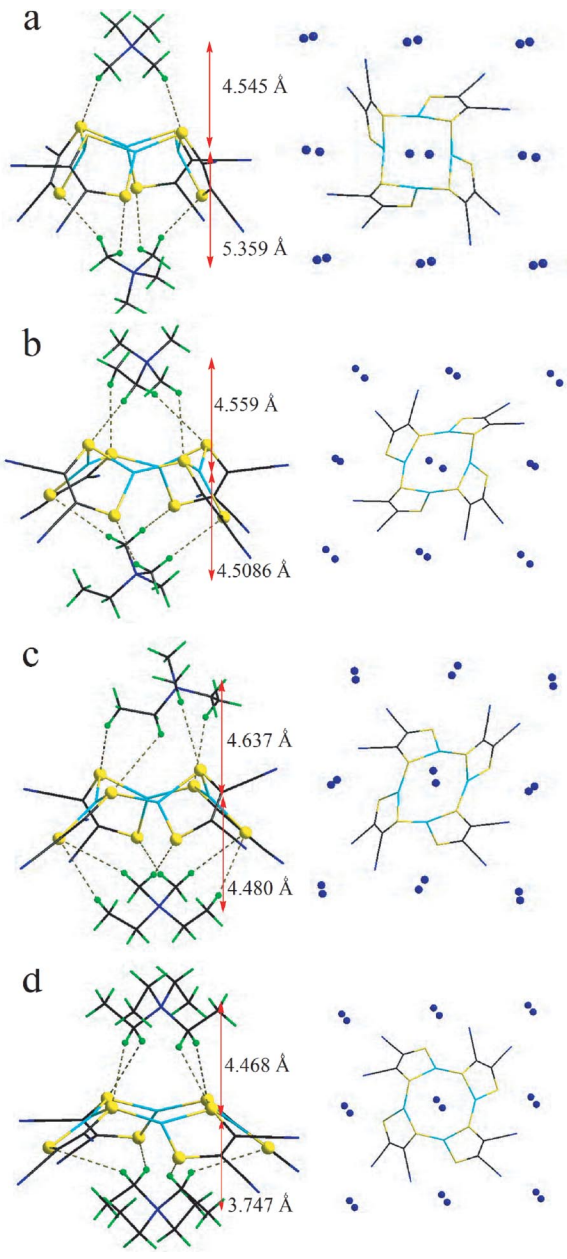

Figure 9. View of the crystal structures of **1** (a), **2** (b), **3** (c), and **5** (d) showing the interactions between the host framework and the cations above and below it; left: hydrogen bonds are shown as broken lines and the position of the cation above and below the virtual Cu_4 plane is indicated by a red arrow; right: those cations in the lattice involved in the formation of H-bonds with S and N atoms of the mnt ligands are shown as blue balls. Color code: C: black; N: blue; S: yellow; Cu: cyan; H: green.

C–H···N ($d_{C–N}$ = 3.18–3.74 Å and ∠C–H···N = 108–177°) interactions, as illustrated in Figure 9. The C–H groups of the $Me_2Et_2N^+$ cations interact with the adjacent S and N of host framework.

The Et_4N^+ ion in compound **5** lies at the center of the two sides of the host framework, which forms C–H···S hydrogen-bonding interactions with the C–H groups of the ¡cation (Figure 9). Moreover, weak C–H···S ($d_{C–S}$ = 3.49–4.03 Å and ∠C–H···S = 122–168°) and C–H···N ($d_{C–N}$ = 3.34–3.73 Å and ∠C–H···N = 107–166°) hydrogen-bonding interactions are found between the host and neighboring cations present in the lattice. These varied interactions with this different tetraalkylammonium cation lead to a different topology.

The distances between the central nitrogen of the bottom cation (inside the partly opened umbrella) in **1**, **2**, **3**, and **5** and the corresponding Cu_4 plane are 5.359, 4.509, 4.480, and 3.747 Å, respectively, which means that the Et_4N^+ cation lies much closer to the Cu_4 plane than any of the other cations studied here. This is due to the four arms of the Et_4N^+ cation acting as a spacer that stretches outward uniformly in four different directions, which causes the umbrella shape to open the most.

It is understandable that such a partly opened umbrella structure will not be stable in solution as solvation forces are likely to overcome the energy of these hydrogen bonds, thereby causing melting in the plasticity of the host. The existence of a hydrophobic surface area and ion-pair and packing interactions are expected in the solid state along with the above-mentioned weak H-bonding. The flexible structure of the anion maps the hydrophobic surface area of the cation in an attempt to maximize the anion/cation surface area interactions. Such a driving force is not expected to be directional like H-bonding, although some orientational effects are expected to occur. Some distortion of the cation may reflect packing interactions with the anion. These forces are individually weak but collectively they dictate a discrete supramolecular entity in the solid state.

Elastic Host-Framework

A significant variation is observed in the core structures with a change in the cations. Figure 10 shows the structural variations in the tetramer found in complexes **1**–**5**. As stated earlier, cations such as Me_4N^+, Me_3EtN^+, $Me_2Et_2N^+$, $MeEt_3N^+$, or Et_4N^+ each occupy the interior of the corresponding partly opened host cavity with another cation present on the opposite side. The changes of the S···S separation should be reflected in the change in cavity size of these complexes. The cavity size, in other words the opening of the umbrella, gradually increases on going from Me_4N^+ to Et_4N^+, and we have calculated the area of the quadrilateral (4S $area_{quad.}$) formed by connecting the midpoints of the sulfur atoms in structures **1**, **2**, **3**, and **5** (20.98, 27.00, 29.68, and 40.36 Å^2, respectively). The size of the cavity depends on the nature of the cation, as the largest cation produces the maximum value of $area_{quad.}$. Thus, there is a 92.34% increase in $area_{quad.}$ for **5** with respect to that of **1**. This effect is reflected in the $\{Cu_4S_4\}$ molecular core, as shown in Figure 10.

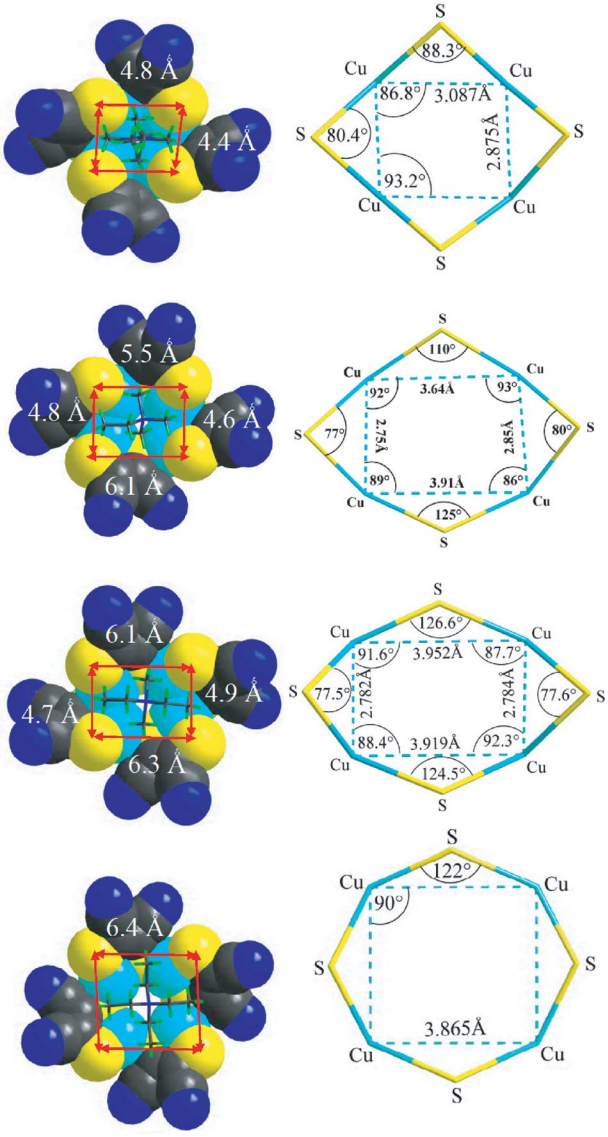

Figure 10. Various tetramer conformations found in **1** (first row), **2** (second row), **3** (third row), and **4** (fourth row); first column: bottom view of the host framework (space-filling model) with one cation (frame-wire model, disordered tetramethyl cation) showing the cavity size and shape; the red arrows show the area of cavity; second column: frame-wire model representing the core structure of the tetramers; the corresponding bond lengths and angles are obtained by considering Cu ions as the vertex of the quadrilaterals. Color code: C: black; N: blue; S: yellow; Cu: cyan; H: green.

The overall shape of the macrocyclic entity could be hypothetically considered to start with the four coplanar copper ions situated at the corners of a quadrilateral. We also calculated the area of the quadrilateral (4Cu-$area_{quad.}$) formed by connecting the midpoints of the copper atoms in **1**, **2**, **3**, and **5** (8.85, 10.56, 11.41, and 14.93 Å^2, respectively). Thus, there is a 68.70% increase in $area_{quad.}$ in **5**

compared to that in **1**. This numerical comparison of the area of these complexes is guided by three principal parameters, which can be explained by considering the reference geometry shown in Figure 11.

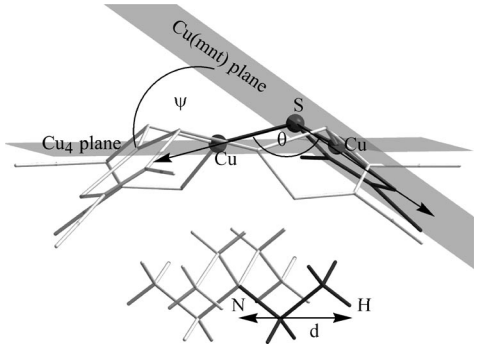

Figure 11. Representation of the geometric parameters: ψ denotes the angle between the Cu(mnt) and Cu_4 planes, θ denotes the angle ($\angle$Cu–S–Cu) at the S atom which bridges two Cu(mnt) units, and d denotes the arm length (alkyl chain) of the cation; the other parts are transparent for clarity.

The three parameters are: (1) the {Cu(mnt)} planes are inclined at an angle (ψ) with the Cu_4 plane; (2) the angle (θ) at the S atom which is linked to two {Cu(mnt)} units; and (3) the length (d) of the arms of the cation. These parameters are related as d is proportional to θ and to $1/\psi$. The angle θ ranges from 76.8° to 126.6° (Table 2) and is greatly affected even by a partial change in the arms of the cation. This gives rise to appreciable variations in the intramolecular Cu···Cu separation, which ranges from 2.753 to 3.952 Å. The four methyl arms of the cation in **1** push the edge of the tetramer in different directions by H-bonding to make two pairs of Cu–S–Cu angles (88.3° and 80.4°), which reflect the corresponding Cu···Cu separations of 2.875 and 3.087 Å, respectively. In **2**, where one of the four arms of the cation increases in length from Me to Et, one of the Cu–S–Cu angles increases to 125.2° (the other three angles are 110.3°, 79.7°, and 76.8°), which means that the maximum Cu···Cu separation increases to 3.905 Å (the other three distances are 3.641, 2.856, and 2.753 Å). In the molecular tetramer of **3**, two of the Cu–S–Cu angles are large (126.6° and 124.5°) and the remaining two angles are small (77.4° and 77.5°) due to the presence of two Et and two Me arms in the cation. As a result, the Cu···Cu separations are 3.952, 3.919, 2.782, and 2.784 Å. The four Cu–S–Cu angles in **5** are the same (122°) and so are the Cu···Cu separations (3.865 Å). This is due to the presence of four equivalent Et arms in the cation.

The μ_2-S bridge behaves like a hinge on a door, therefore the Cu–S distance does not contribute to the structural variability. It is important to recognize that it is only within the elastic limit of the host frame that various guests can find suitable linkers for an adaptable overall geometry. The size and shape of the frameworks are governed by the cation,[30] therefore the cation plays a decisive role in deciding the structure in the solid state. A 2D projection view (the four terminal H-atoms from four arms point vertically in the virtual 4S-plane) of the cation taken from the 3D geometry is shown in Figure 12 to clarify the situation.

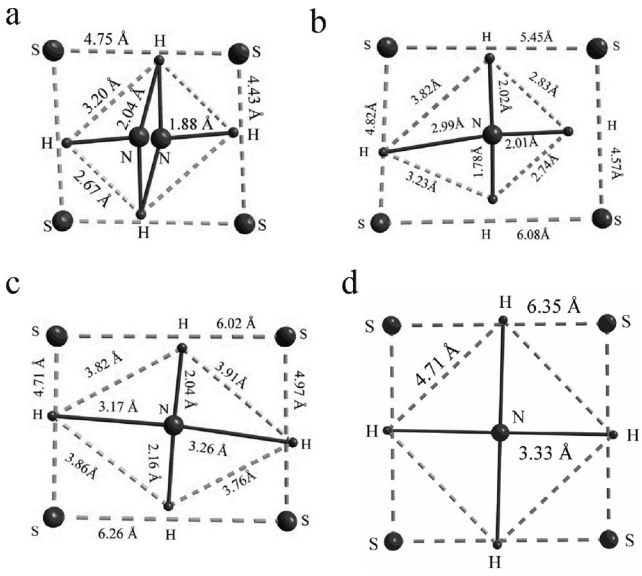

Figure 12. Projection view of four terminal H-atoms from four arms of the cation and four μ-S atoms of the host framework in the 2D plane (virtual 4S plane, taken from 3D geometry). The blueprint of the size and shape of the cation and length of the carbon chain (arm) are shown by solid lines: (a) disordered tetramethylammonium cation (almost rectangular), (b) trimethylethylammonium cation (parallelogram), (c) diethyldimethylammonium cation (close to rectangular), (d) tetraethylammonium cation (perfect square).

The overall dimension and shape of the cation can therefore be extracted by considering the four coplanar H-atoms to be at the corners of a hypothetical quadrilateral. The blueprint of Me_4N^+ is a distorted square geometry (due to the special position disorder of the N-atom in lattice) with dimensions of 3.203×2.675 Å^2 and angles that deviate slightly from 90° (94.1° and 85.9°). Et_4N^+ resembles a perfect square with dimensions of 4.701×4.701 Å^2 and all the angles being 90°, whereas $Me_2Et_2N^+$ resembles a rectangle

Table 2. Structural parameters of **1**–**5**.

Complexes	d[a] [Å]	θ ($\angle$Cu–S–Cu) [°]	ψ [°]	Cu···Cu [Å]
1	4 Me	88.3 and 80.4	65.1 and 59.9	2.875 and 3.087
2	3 Me and Et	110.3, 125.2, 79.7 and 76.8	62.9, 55.3, 57.7 and 41.4	3.641, 3.905, 2.846 and 2.753
3	2 Me and 2 Et	126.6, 124.5, 77.4 and 77.5	56.8, 47.6, 58.5 and 39.9	3.952, 3.919, 2.784 and 2.782
5	4 Et	122	36.4	3.865

[a] Substituents in the tetraalkylammonium cation.

with sides of 3.815, 3.906, 3.857, and 3.764 Å and angles of 66.3°, 112.5°, 66.3° and 114.8°, and Me_3EtN^+ resembles a parallelogram with sides of 3.821, 2.834, 2.741, and 3.229 Å and angles of 96.2°, 85.9°, 113.3°, and 64.6°. The 4S-base of the host and the 4H base of the guest are oriented face-to-face with a rotation angle of close to 90°. These sizes and shapes of the host framework are in agreement with expectations based on the size[31] and shape of the cations, therefore the structural design information[32] stored in a cation is transferred to the host framework through H-bonding to yield a specific supramolecular entity. This work unambiguously proves that how a discrete $\{Cu_4S_4\}$ framework responds to the inclusion of a guest depends on the nature of the guest. More interestingly, and contrary to common host-guest assemblies, the present framework demonstrates elasticity by shrinking and expanding to accommodate guests of varying sizes and shapes.

Conclusions

This work illustrates the power of a guest cation to determine the final shape of some supramolecular species in the solid state. The host anion is relaxed in solution and behaves like melted plastic, i.e., free from any rigid shape. The guest molds the shape of the cavity of the melted elastic host due to its size and shape and the host then solidifies during the crystallization process and assumes a rigid plastic shape. The molecular structural design information that is stored in the cation is therefore transferred to the host framework through H-bonding to yield a specific supramolecular entity. The combined UV/Vis, NMR, CV, and ESI-MS results confirm that all these designed structures are lost in solution, which means that guest encapsulation and guest exchange become possible by taking advantage of the plasticity in the solid state and the elasticity in solution.

Experimental Section

Materials: All manipulations were carried out under argon using Schlenk-line techniques. $Na_2(mnt)$ was prepared by the literature method,[33] as was diethyldimethylammonium bromide.[34] Freshly prepared[35] CuCl was used in the synthesis. Ethyltrimethylammonium iodide, tetramethylammonium bromide, triethylmethylammonium bromide, and tetraethylammonium bromide were purchased from Aldrich and used without further purification.

Physical Measurements: Cyclic voltammetry (CV) and differential pulse polarography (DPP) were performed with an Epsilon EC-20 machine. The electrolytic cell used was a conventional three-compartment cell with a GCE working electrode, a Pt auxiliary electrode, and an Ag/AgCl reference electrode. The CV measurements were performed at room temperature using 0.1 M KPF_6 as the supporting electrolyte in CH_3CN at a scan rate of 100 mV s^{-1}. The ferrocenium/ferrocene couple was used as the internal standard (E_0 = 0.53 V under these conditions). Electronic absorption spectra were measured with the help of a USB2000 UV/Vis Spectrometer. ^{13}C NMR spectra were recorded with a JEOL JNM-LA 400 FT-NMR machine. The negative mode ESI mass spectra were recorded with a Waters Micromass Q TOF Premier Mass Spectrometer. The samples (dissolved in acetonitrile) were introduced into the ESI source with a syringe pump at the rate of 5 μL per minute; the ESI capillary voltage was set to 3.5 or 2.5 kV and the cone voltage was 40 V. Theoretical isotope ratio calculations were performed using the program ISOPRO3.[20] Far-infrared spectra were recorded for CsI pellets in the range 200–400 cm^{-1} and IR spectra were recorded for KBr pellets in the range 400–4000 cm^{-1} with a Bruker Vertex 70 FT-IR spectrophotometer. Elemental analyses for carbon, hydrogen, nitrogen and sulfur analysis were determined with a Perkin–Elmer 2400 microanalyser.

General Procedure for the Synthesis of Complexes 1–5: Solid CuCl (0.99 g, 10 mmol) was added to a solution of $Na_2(mnt)$ (1.86 g, 10 mmol) in 80 mL of H_2O and the mixture was stirred for 30 min to dissolve the solid. An excess of the corresponding tetraalkylammonium salt [Me_4NBr (**1**), Me_3EtNI (**2**), Me_2Et_2NBr (**3**), $MeEt_3NBr$ (**4**), and Et_4NBr (**5**)] was added to the solution to precipitate a yellow solid, which was collected by filtration, washed with H_2O and 2-propanol, and finally with diethyl ether. Diffraction-quality crystals were obtained by diffusion of diethyl ether vapor into an acetonitrile solution of the crude product.

$[Me_4N]_4[Cu_4(mnt)_4]$ (1): Orange crystals, m.p. 232–234 °C, yield 2.28 g (82%). $C_{32}H_{48}Cu_4N_{12}S_8$ (1111.6): calcd. C 34.55, H 4.32, N 15.11, S 23.03; found C 34.50, H 4.29, N 15.12, S 22.97. IR (KBr): $\tilde{\nu}$ = 2190 cm^{-1} [ν(C≡N)]. FT far-IR (CsI): $\tilde{\nu}$ = 280 cm^{-1} [ν(Cu–S)]. UV/Vis: λ (ε) = 377 nm (46195 $M^{-1}cm^{-1}$), 266 (36275). ESI-MS: *m/z* 1035.81 $[Me_4N]_3[Cu_4(mnt)_4]^-$. ^{13}C NMR ([D$_6$]DMSO): δ = 124.67 (CN), 120.12 (C=C), 59.48 ppm (CH_3).

$[Me_3EtN]_4[Cu_4(mnt)_4]$ (2): Orange crystals, m.p. 220–222 °C, yield 2.39 g (82%). $C_{36}H_{56}Cu_4N_{12}S_8$ (1167.7): calcd. C 36.99, H 4.79, N 14.39, S 21.93; found C 36.97, H 4.74, N 14.32, S 21.95. IR (KBr): $\tilde{\nu}$ = 2190 cm^{-1} ν(C≡N). FT-far-IR (CsI): 279 cm^{-1} [ν(Cu–S)]. UV/Vis: λ (ε) =377 nm (46185 $M^{-1}cm^{-1}$), 266 (36257). ESI-MS: *m/z* 1077.94 $[Me_3EtN]_3[Cu_4(mnt)_4]^-$. ^{13}C NMR ([D$_6$]DMSO): δ = 124.67 (CN), 120.12 (C=C), 60.94 (α-CH_2), 51.73 (CH_3), 8.16 ppm (β-CH_3).

$[Me_2Et_2N]_4[Cu_4(mnt)_4]$ (3): Orange crystals, m.p. 201–203 °C, yield 2.54 g (83%). $C_{40}H_{64}Cu_4N_{12}S_8$ (1223.8): calcd. C 39.23, H 5.23, N 13.73, S 20.92; found C 38.99, H 5.21, N 13.75, S 20.94. IR (KBr): $\tilde{\nu}$ = 2190 cm^{-1} [ν(C≡N)]. FT-far-IR (CsI): $\tilde{\nu}$ = 276 cm^{-1} [ν(Cu–S)]. UV/Vis: λ (ε) =377 nm (46177 $M^{-1}cm^{-1}$), 266 (36263). ESI-MS: *m/z* 1119.87 $[Me_2Et_2N]_3[Cu_4(mnt)_4]^-$. ^{13}C NMR ([D$_6$]DMSO): δ = 124.67 (CN), 120.12 (C=C), 58.04 (α-CH_2), 48.99 (CH_3), 7.83 ppm (β-CH_3).

$[MeEt_3N]_4[Cu_4(mnt)_4]$ (4): Yellowish orange crystals, m.p. 189–191 °C, yield 2.72 g (85%). $C_{44}H_{72}Cu_4N_{12}S_8$ (1279.9): calcd. C 41.25, H 5.62, N 13.13, S 20.00; found C 41.28, H 5.58, N 13.10, S 19.98. IR (KBr): $\tilde{\nu}$ = 2190 cm^{-1} [ν(C≡N)]. FT-far-IR (CsI): $\tilde{\nu}$ = 278 cm^{-1} [ν(Cu–S)]. UV/Vis: λ (ε) =377 nm (46159 $M^{-1}cm^{-1}$), 266 (36235). ESI-MS: *m/z* 1161.84 $[MeEt_3N]_3[Cu_4(mnt)_4]^-$. ^{13}C NMR ([D$_6$]DMSO): δ = 124.67 (CN), 120.12 (C=C), 53.71 (α-CH_2), 50.33 (CH_3), 11.34 ppm (β-CH_3).

$[Et_4N]_4[Cu_4(mnt)_4]$ (5): Yellow crystals, m.p. 178–180 °C, yield 2.84 g (85%). $C_{48}H_{80}Cu_4N_{12}S_8$ (1335.9): calcd. C 43.11, H 5.99, N 12.57, S 19.16; found C 43.09, H 5.98, N 12.55, S 19.13. IR (KBr): $\tilde{\nu}$ = 2190 cm^{-1} [ν(C≡N)]. FT-far-IR (CsI): $\tilde{\nu}$ = 279 cm^{-1} [ν(Cu–S)]. UV/Vis: λ (ε) =377 nm (46195 $M^{-1}cm^{-1}$), 266 (36245). ESI-MS: *m/z* 1203.99 $[Et_4N]_3[Cu_4(mnt)_4]^-$. ^{13}C NMR ([D$_6$]DMSO): δ = 124.67 (CN), 120.12 (C=C), 51.49 (α-CH_2), 7.15 ppm (β-CH_3).

Preparation of $[Et_4N][Cu(mnt)(PPh_3)]$ (6): Compound **5** (0.34 g, 0.25 mmol) and PPh_3 (0.27 g, 1.2 mmol) were added to 40 mL of dichloromethane and the mixture stirred for about 5 min to give a

Table 3. Crystallographic data and refinement details for complexes **1**–**3**, **5**, and **6**.

Compounds	**1**	**2**	**3**	**5**	**6**
Empirical formula	$C_{32}H_{48}Cu_4N_{12}S_8$	$C_{36}H_{56}Cu_4N_{12}S_8$	$C_{40}H_{64}Cu_4N_{12}S_8$	$C_{48}H_{80}Cu_4N_{12}S_8$	$C_{30}H_{35}CuN_3PS_2$
Formula weight	1111.58	1167.69	1223.79	1335.88	596.27
Temperature [K]	100(2)	100(2)	100(2)	100(2)	100(2)
Crystal system	monoclinic	triclinic	monoclinic	tetragonal	monoclinic
Space group	*C*2/*c*	$P\bar{1}$	$P2_1/c$	*P*4/*n*	$P2_1/n$
a [Å]	13.379(5)	13.279(5)	14.730(5)	14.158(5)	11.648(5)
b [Å]	27.810(5)	14.144(5)	28.028(5)	14.158(5)	11.579(5)
c [Å]	13.075(5)	15.524(5)	13.408(5)	15.044(5)	22.173(5)
α [°]	90	64.226(5)	90	90	90
β [°]	94.773(5)	87.667(5)	97.053(5)	90	94.679(5)
γ [°]	90	82.496(5)	90	90	90
Volume [Å^3]	4848(3)	2602.7(16)	5494(3)	3015.6(18)	2980.6(19)
Z	4	2	4	2	4
D_c [Mg m^{-3}]	1.523	1.490	1.480	1.471	1.329
μ [mm^{-1}]	2.113	1.969	1.872	1.712	0.950
F(000)	2272	1200	2528	1392	1248
θ range [°]	2.14–28.32	2.11–28.32	2.07–28.34	1.98–28.33	1.99–28.31
Independent reflections (collected)	6004(16172)	12419(17494)	13580(36819)	3761(19978)	7359(19617)
Goodness-of-fit on F^2	1.159	1.048	1.040	1.295	1.023
Final *R* indices [$I > 2\sigma(I)$] R_1,[a] (wR_2)[b] [%]	0.0437 (0.0890)	0.0878 (0.1912)	0.0864 (0.1925)	0.0768 (0.1633)	0.0460 (0.1037)

[a] $R_1 = \Sigma||F_o| - |F_c||/\Sigma|F_o|$. [b] $wR_2 = \{\Sigma[w(F_o^2 - F_c^2)^2]/\Sigma[w(F_o^2)^2]\}^{1/2}$.

clear, light yellow solution. Addition of petroleum ether afforded **6** as a pale-yellow crystalline product, which was collected by filtration and washed with petroleum ether. Single crystals suitable for X-ray structure analysis were grown by slow diffusion of petroleum ether into a dichloromethane solution, yield 0.54 g (90%), m.p. 159–161 °C. $C_{30}H_{35}CuN_3PS_2$ (596.27): calcd. C 60.38, N 7.04, H 5.87, S 10.73; found C 60.40, N 7.00, H 5.89, S 10.71. IR (KBr): $\tilde{\nu}$ = 2190 cm^{-1} [ν(C≡N)]. FT-far-IR (CsI): $\tilde{\nu}$ = 277 cm^{-1} [ν(Cu–S)]. UV/Vis: λ (ε) =372 nm (11305 M^{-1}cm^{-1}). ESI-MS: *m*/*z* 465 [Cu(mnt)PPh$_3$]$^-$. ^{13}C NMR ([D$_6$]DMSO, δ): δ = 133.48 (1-Ph), 130.60 (*o*-CH of Ph), 129.11 (*m*,*p*-CH of Ph), 125.21 (CN), 120.86 (C=C), 51.55 (α-CH$_2$), 7.16 ppm (β-CH$_3$).

X-ray Crystallographic Data Collection and Refinement of Structures: Single crystals of **1**–**6** suitable for X-ray diffraction measurements were obtained by slow diffusion of diethyl ether vapor into a solution of the respective complex in acetonitrile X-ray data were collected on a Bruker SMART APEX CCD-based X-ray diffractometer equipped with a CCD area detector. Data were collected using graphite-monochromated Mo-K_α radiation (λ = 0.71069 Å) at low temperature (100 K). All empirical absorption corrections were applied using the SADABS program.[36] Cell constants were obtained from the least-squares refinement of three-dimensional centroids through the use of CCD recording of narrow ω rotation frames, completing almost all-reciprocal space in the stated θ range. All data were collected with SMART 5.628 (Bruker, 2003), and were integrated with the Bruker SAINT[37] program. Each structure was solved using SIR-97 and refined using SHELXL-97.[38] The space group of each compound was determined based on the lack of systematic absences and intensity statistics. Full-matrix least-squares/difference and Fourier cycles were performed to locate the remaining non-hydrogen atoms. All non-hydrogen atoms were refined with anisotropic displacement parameters. Some carbon atoms of the ethyl groups of the cations were disordered for **2**, **3**, and **5**; these atoms were refined with the free part instruction in SHELXL-97. Additional crystallographic calculations were performed with the PLATON[39] program suite. Further details of the crystallographic data and refinement parameters are provided in Table 3.

CCDC-668698 (for **5**), -668699 (for **2**), -668700 (for **1**), -668701 (for **6**), -668702 (for **3**) contain the supplementary crystallographic data for this paper. These data can be obtained free of charge from The Cambridge Crystallographic Data Center via www.ccdc.cam.ac.uk/data_request/cif.

Supporting Information (see also the footnote on the first page of this article): UV/Vis spectra of $[Et_4N]_4[Cu_4(mnt)_4]$, $[Et_4N]_4[Cu_8(mnt)_6]$, and $[Et_4N]_2[Cu^{II}(mnt)_2]$ (Figure S1); CV of $[Et_4N]_4[Cu_4(mnt)_4]$ at platinum and glassy carbon disc electrodes in the scan range 50–400 mV s^{-1} (Figure S2); CV (repetitive scan) of $[Et_4N]_4[Cu_4(mnt)_4]$ (Figure S3); theoretical and experimental (ESI-MS) isotopic distribution patterns of the parent ion peak for $[Me_4N]_3[Cu_4(mnt)_4]^-$ (Figure S4), $[Me_4EtN]_3[Cu_4(mnt)_4]^-$ (Figure S5), $[Me_2Et_2N]_3[Cu_4(mnt)_4]^-$ (Figure S6), $[MeEt_3N]_3[Cu_4(mnt)_4]^-$ (Figure S7); theoretical and experimental (ESI-MS) isotopic distribution patterns of the ion peak for $[Et_4N]_2[Cu_3(mnt)_3]^-$ (Figure S8), $[Et_4N][Cu_2(mnt)_2]^-$ (Figure S9), $[Cu(mnt)]^-$ (Figure S10); XRD pattern of $[Et_4N]_4[Cu_4(mnt)_4]$ (Figure S11); far-FT-IR spectra of **1**–**6** (Figure S12).

Acknowledgments

B. K. M. and K. P. gratefully acknowledge senior doctoral fellowships from the UGC and the CSIR, New Delhi, respectively, and S. S. thanks the DST, New Delhi, for a research grant.

[1] a) J.-M. Lehn, *Supramolecular Chemistry: Concepts and Perspectives*, VCH, Weinheim, **1995**; b) R. F. Saalfrank, B. Demleitner, in *Transition Metals in Supramolecular Chemistry*, John Wiley, New York, **1999**, p. 1–51; c) S. Leininger, B. Olenyuk, P. J. Stang, *Chem. Rev.* **2000**, *100*, 853; d) Q. H. Yuan, L.-J. Wan, H. Jude, P. J. Stang, *J. Am. Chem. Soc.* **2005**, *127*, 16279; e) L. H. Uppadine, J.-M. Lehn, *Angew. Chem. Int. Ed.* **2004**, *43*, 240; f) M. Ruben, J. Rojo, F. J. Romero-Salguero, L. H. Uppadine, J.-M. Lehn, *Angew. Chem. Int. Ed.* **2004**, *43*, 3644; g) J. L. Atwood, L. J. Barbour, S. J. Dalgarno, M. J. Hardie, C. L. Raston, H. R. Webb, *J. Am. Chem. Soc.* **2004**, *126*, 13170; h) Y. K. Kryschenko, S. R. Seidel, A. M. Arif, P. J. Stang, *J.*

Am. Chem. Soc. **2003**, *125*, 5193; i) C. J. Kuehl, Y. K. Kryshenko, U. Radhakrishnan, S. R. Seidel, S. D. Huang, P. J. Stang, *Proc. Natl. Acad. Sci. USA* **2002**, *99*, 4932; j) N. S. Oxtoby, A. J. Blake, N. R. Champness, C. Wilson, *Proc. Natl. Acad. Sci. USA* **2002**, *99*, 4905; k) S. B. T. Nguyen, D. L. Gin, J. T. Hupp, X. Zhang, *Proc. Natl. Acad. Sci. USA* **2001**, *98*, 11849; l) G. F. Swiegers, T. J. Malefetse, *Chem. Rev.* **2000**, *100*, 3483; m) R. D. Schnebeck, E. Freisinger, B. Lippert, *Angew. Chem. Int. Ed.* **1999**, *38*, 168; n) M. Fujita, *Acc. Chem. Res.* **1999**, *32*, 53; o) F. A. Cotton, L. M. Daniels, C. Lin, C. A. Murillo, *J. Am. Chem. Soc.* **1999**, *121*, 4538; p) M. Fujita, M. Aoyagi, F. Ibukuro, K. Ogura, K. Yamaguchi, *J. Am. Chem. Soc.* **1998**, *120*, 611; q) M. Fujita, F. Ibukuro, K. Yamaguchi, K. Ogura, *J. Am. Chem. Soc.* **1995**, *117*, 4175.

[2] a) N. Gimeno, R. Vilar, *Coord. Chem. Rev.* **2006**, *250*, 3161; b) C. S. Campos-Fernández, B. L. Schottel, H. T. Chifotides, J. K. Bera, J. Bacsa, J. M. Koomen, D. H. Russell, K. R. Dunbar, *J. Am. Chem. Soc.* **2005**, *127*, 12909; c) R. L. Paul, R. Z. Bell, J. C. Jeffery, J. A. McCleverty, M. D. Ward, *Proc. Natl. Acad. Sci. USA* **2002**, *99*, 4883; d) C. S. Campos-Fernández, R. Clérac, J. M. Koomen, D. H. Russell, K. R. Dunbar, *J. Am. Chem. Soc.* **2001**, *123*, 773; e) B. Hasenknopf, J.-M. Lehn, K. B. O. Neisel, G. Baum, D. Fenske, *Angew. Chem. Int. Ed. Engl.* **1996**, *35*, 1838.

[3] a) M. Scherer, D. L. Caulder, W. Johnson, K. N. Raymond, *Angew. Chem. Int. Ed.* **1999**, *38*, 1588; b) D. L. Caulder, R. E. Power, T. N. Parac, K. N. Raymond, *Angew. Chem. Int. Ed.* **1998**, *37*, 1840; c) R. W. Saalfrank, R. Burak, A. Breit, D. Stalke, R. Herbst-Irmer, J. Daub, M. Porch, E. Bill, M. Muether, A. Trautwein, *Angew. Chem. Int. Ed. Engl.* **1994**, *33*, 1621.

[4] J.-M. Lehn, *Chem. Soc. Rev.* **2007**, *36*, 151.

[5] K. Mueller-Dethlefs, P. Hobza, *Chem. Rev.* **2000**, *100*, 143.

[6] a) D. L. Caulder, K. N. Raymond, *Acc. Chem. Res.* **1999**, *32*, 975; b) C. Jones, *Chem. Soc. Rev.* **1998**, *27*, 289; c) P. Jacopozzi, E. Dalcanale, *Angew. Chem. Int. Ed. Engl.* **1997**, *36*, 613; d) M. Morgan, J. Rebek Jr, *Chem. Rev.* **1997**, *97*, 1647.

[7] a) D. P. Michael, K. N. Raymond, *Chem. Soc. Rev.* **2007**, *36*, 161; b) B. E. F. Tiedemann, K. N. Raymond, *Angew. Chem. Int. Ed.* **2006**, *45*, 83; c) F. W. B. Van Leeuwen, A. L. Spek, H. Kooijman, M. Crego-Calama, D. N. Reinhoudt, *Angew. Chem. Int. Ed.* **2003**, *42*, 5717; d) S. C. N. Hsu, M. Ramesh, J. H. Espenson, T. B. Rauchfuss, *Angew. Chem. Int. Ed.* **2003**, *42*, 2663; e) S. L. Craig, S. Lin, J. Chen, J. Rebek Jr, *J. Am. Chem. Soc.* **2002**, *124*, 8780; f) W.-Y. Sun, T. Kusukawa, M. Fujita, *J. Am. Chem. Soc.* **2002**, *124*, 11570; g) J. L. Atwood, A. Szumna, *J. Am. Chem. Soc.* **2002**, *124*, 10646; h) J. Santamaría, T. Martín, G. Hilmersson, S. L. Craig, J. Rebek Jr, *Proc. Natl. Acad. Sci. USA* **1999**, *96*, 8344.

[8] A. V. Davis, K. N. Raymond, *J. Am. Chem. Soc.* **2005**, *127*, 7912.

[9] a) P. S. Mukherjee, N. Das, Y. K. Kryschenko, A. M. Arif, P. J. Stang, *J. Am. Chem. Soc.* **2004**, *126*, 2464 and references cited therein; b) C.-Y. Su, Y.-P. Cai, C.-L. Chen, M. D. Smith, W. Kaim, H.-C. zur Loye, *J. Am. Chem. Soc.* **2003**, *125*, 8595; c) D. L. Caulder, C. Brulckner, R. E. Powers, S. Kolnig, T. N. Parac, J. A. Leary, K. N. Raymond, *J. Am. Chem. Soc.* **2001**, *123*, 8923.

[10] a) G. Henkel, B. Krebs, *Chem. Rev.* **2004**, *104*, 801; b) I. G. Dance, *Polyhedron* **1986**, *5*, 1037.

[11] H. Dietrich, W. Storck, G. Manecke, *Makromol. Chem.* **1981**, *182*, 2371.

[12] a) S. Perruchas, K. Boubekeur, *Dalton Trans.* **2004**, 2394; b) H. Dietrich, *Acta Crystallog. Sect. A* **1978**, *32*, S26; c) F. J. Hollander, D. Coucouvanis, *J. Am. Chem. Soc.* **1977**, *99*, 6268; d) F. J. Hollander, D. Coucouvanis, *J. Am. Chem. Soc.* **1974**, *96*, 5647; e) L. E. McCandish, E. C. Bissel, D. Coucouvanis, J. P. Fackler Jr, K. Knox, *J. Am. Chem. Soc.* **1968**, *90*, 7357.

[13] R. Hesse, *Ark. Kemi.* **1963**, *20*, 481.

[14] S. L. Lawton, R. W. J. Ohrbaugh, G. T. Kokotailo, *Inog. Chem.* **1972**, *11*, 612.

[15] A. Camus, N. Marsich, *Inorg. Chim. Acta* **1989**, *161*, 87.

[16] C. W. Liu, R. J. Staples, J. P. Fackler, *Coord. Chem. Rev.* **1998**, *174*, 147.

[17] B. K. Maiti, K. Pal, S. Sarkar, *Dalton Trans.* **2008**, 1003.

[18] a) X. Xue, X.-S. Wang, R.-G. Xiong, X.-Z. You, B. F. Abrahams, C.-M. Che, *Angew. Chem. Int. Ed.* **2002**, *41*, 2944; b) Y. Shimazaki, H. Yokiyama, O. Yamauchi, *Angew. Chem. Int. Ed.* **1999**, *38*, 2401.

[19] U. N. Andersen, G. Seeber, D. Fiedler, K. N. Raymond, *J. Am. Soc. Mass Spectrom.* **2006**, *17*, 292.

[20] M. Senko, *ISOPRO 3.0*; Sunnyvale, CA (http://members.aol.-com/msmssoft).

[21] M. T. Garland, J.-F. Halet, J.-Y. Saillard, *Inorg. Chem.* **2001**, *40*, 3342.

[22] D. Nasipuri, *Stereochemistry of Organic Compounds: Principles*, and Applications, John Wiley & Sons, New York, **1991**.

[23] B. L. Hathaway, *Comprehensive Coordination Chemistry* (Eds.: G. Wilkinson), Pergamon, Oxford, England, **1987**, vol. 5, p. 533. The copper–sulfur bond lengths are dependent on the coordination number of the copper atom and distinct ranges can be distinguished: 2.14–2.17 Å for two-coordinate copper atoms, 2.22–2.23 Å for three-coordinate copper atoms, and 2.33–2.48 Å for four-coordinate copper atoms.

[24] a) B. K. Maiti, K. Pal, S. Sarkar, *Eur. J. Inorg. Chem.* **2007**, 5548; b) B. K. Maiti, K. Pal, S. Sarkar, *Inorg. Chem. Comun.* **2004**, *7*, 1027; c) J. R. Nicholson, I. L. Abrahams, W. Clegg, C. D. Garner, *Inorg. Chem.* **1985**, *24*, 1092; d) G. A. Bowmaker, G. R. Clark, I. G. Dance, *Polyhedron* **1983**, *2*, 1031; e) D. Coucouvanis, C. N. Murphy, S. K. Kanodia, *Inorg. Chem.* **1980**, *19*, 2993.

[25] Crystals of **4** are monoclinic, space group *P*4/*n*, with a = 14.089(5), b = 14.089(5), c = 14.692(5) Å, α = 90°, β = 90° and γ = 90°. They give weak, poor quality diffraction data (despite repeated recrystallization and data collection), and the structure could not be satisfactorily refined.

[26] a) M. Takuma, Y. Ohki, K. Tatsumi, *Inorg. Chem.* **2005**, *44*, 6034; b) S. Zeltner, S. Jelonek, J. Sieler, R.-M. Olk, *Eur. J. Inorg. Chem.* **2001**, 1535.

[27] a) K. Nakamoto, *Infrared and Raman Spectra of Inorganic and Coordination Compounds*, 4th ed., John Wiley & Sons, New York, **1986**, p. 101; b) R. C. Bott, G. A. Bowmaker, C. A. Davis, G. A. Hope, B. E. Jones, *Inorg. Chem.* **1998**, *37*, 651; c) K. Fujisawa, S. Imai, N. Kitajima, Y. Moro-oka, *Inorg. Chem.* **1998**, *37*, 168.

[28] a) G. R. Dessiraju, T. Steiner, *The Weak Hydrogen Bond*, in *Structural Chemistry and Biology*, Oxford University Press, New York, **1999**; b) G. R. Desiraju, *Crystal Engineering: The Design of Organic Solids*, Elsevier, Amsterdam, **1989**.

[29] a) A. Ikezaki, M. Nakamura, *Inorg. Chem.* **2003**, *42*, 2301; b) G. R. Lewis, I. Dance, *J. Chem. Soc., Dalton Trans.* **2000**, 3176; c) R. Taylor, O. Kennard, *J. Am. Chem. Soc.* **1982**, *104*, 5063.

[30] a) D. M. P. Mingos, A. L. Rohl, *Inorg. Chem.* **1991**, *30*, 3769; b) D. M. P. Mingos, A. Rohl, *J. Chem. Soc., Dalton Trans.* **1991**, 3419.

[31] M. Albrecht, B. O. Blau, R. Froehlich, *Proc. Natl. Acad. Sci. USA* **2002**, *99*, 4867.

[32] a) D. P. Funeriu, K. Rissanen, J.-M. Lehn, *Proc. Natl. Acad. Sci. USA* **2001**, *98*, 10546; b) J.-M. Lehn, *Chem. Eur. J.* **2000**, *6*, 2097; c) D. P. Funeriu, J.-M. Lehn, K. M. Fromm, D. Fensk, *Chem. Eur. J.* **2000**, *6*, 2103.

[33] a) E. I. Stiefel, L. E. Bennett, Z. Dori, T. H. Crawford, C. Simo, H. B. Gray, *Inorg. Chem.* **1970**, *9*, 281; b) A. Davison, R. H. Holm, *Inorg. Synth.* **1967**, *10*, 8; c) G. Bahr, B. Schleitzer, *Chem. Ber.* **1955**, *88*, 1771; d) G. Bahr, *Angew. Chem.* **1956**, *68*, 525.

[34] a) S. Busia, M. Lahtinen, H. Mansikkamäki, J. Valkonena, K. Rissanen, *J. Solid State Chem.* **2005**, *178*, 1722; b) J. Ropponen,

M. Lahtinen, S. Busi, M. Nissinen, E. Kolehmainen, K. Rissanen, *New J. Chem.* **2004**, *28*, 1426.
[35] G. Brauer, *Handbook of Preparative Inorganic Chemistry*, Academic Press, **1965**, vol. 2.
[36] G. M. Sheldrick, *SADABS, Program for Siemens area detector absorption correction*, University of Göttingen, Germany, **1996**.
[37] *SAINT, Program for area detector absorption correction*, Siemens Analytical X-ray Instruments Inc., Madison, WI, **1994**–**1996**.
[38] a) G. M. Sheldrick, *SHELXS97, A Program for the Solution of Crystal Structures from X-ray Data*, University of Göttingen, Germany, **1997**; b) G. M. Sheldrick, *SHELXL97*, *A Program for the Refinement of Crystal Structures from X-ray Data*, University of Göttingen, Germany, **1997**.
[39] a) A. L. Spek, *PLATON*, University of Utrecht, The Netherlands, **2001**; b) A. L. Spek, *Acta Crystallogr.* **1990**, *4*, 194.
Received: January 25, 2008
Published Online: April 15, 2008

